Mem. S.A.It. Vol. 92, 38
© SAIt 2021
Memorie della

SCALA: an innovative external flux calibration device

S. Lombardo[1], D. Küsters[2,3,4], M. Kowalski[4,6], and G. Aldering[3,5]

[1] Aix Marseille Univ, CNRS, CNES, LAM, Marseille, France
[2] Department of Physics, University of California at Berkeley, 366 LeConte Hall MC 7300, Berkeley, CA, 94720-7300
[3] Berkeley Center for Cosmological Physics
[4] Deutsches Elektronen-Synchrotron, D-15735 Zeuthen, Germany
[5] Physics Division, Lawrence Berkeley National Laboratory, 1 Cyclotron Road, Berkeley, CA, 94720
[6] Institut für Physik, Humboldt-Universität zu Berlin, Newtonstraße 15, 12489 Berlin, Germany
e-mail: simona.lombardo@lam.fr

Abstract. Systematic uncertainties in the flux calibration are becoming the limiting factor for the scientific yield of current and future optical surveys. Type Ia supernova (SN Ia) cosmology programs, where an improved calibration directly translates into improved cosmological constraints, are greatly impacted by this. Current methodology rests on models of stars. Here we show how to obtain flux calibration that is traceable to state-of-the-art detector-based calibration. We present the SNIFS Calibration Apparatus (SCALA), a color (relative) flux calibration system developed for the SuperNova Integral Field Spectrograph (SNIFS), operating at the University of Hawaii 2.2 m (UH88) telescope. The SCALA calibration unit is fully deployed since 2015. We show that we can determine the light emitted by SCALA with a long-term repeatability better than 1%. We describe the calibration methodology developed to control for system aging and we present measurements of the SNIFS throughput as estimated by SCALA observations.

Key words. telescopes – instrumentation: miscellaneous – standards – methods: data analysis

1. Introduction

The requirements posed by modern cosmology on precision and accuracy puts more stringent constraints on the ability to convert instrumental signals onto a physical flux scale. One important case is the use of the distance-redshift relation of Type Ia supernovae (SNe Ia) to derive the properties of the Universe, such as the dark energy equation of state parameter, w. In this case, an accurate "absolute color" calibration is what matters most, as one obtains the cosmological parameters by comparing the luminosity of a given restframe wavelength region (usually the Johnson B-band) of the SN Ia spectral energy distribution (SED), at various redshifts. Beyond the establishment of an absolute color calibration, existing SN Ia cosmology data consist of imaging through

$\sim$ 5 filters whose responses as a function of wavelength must also be established in order to transfer absolute color calibration to SNe at different redshifts. The mapping of standard star fluxes to SNe when using filters is not unique; the signals to be compared are integrals of standard star or SN fluxes over a bandpass. SNe have complex spectra over the wavelength ranges spanned by broadband filters. In addition, bandpasses may change with time. Furthermore, any ground-based instrument that uses these standards will also need to correctly account for atmospheric extinction across their bandpasses. That low- and high-redshift SNe are usually observed with completely different telescopes, instruments, and filter sets adds to the difficulty. Thus, it is not surprising that measurements based on current SN Ia cosmology samples are dominated by calibration systematic uncertainties, directly impacting the error on the measured value of w (Betoule et al. 2013, 2014).

There have been several attempts in the past to establish an accurate and reliable calibration system to be used as reference by every observer. For the optical wavelengths, the early work in this direction were reaching calibration accuracies around 2% and were based on comparisons of the Sun, or bright stars such as Vega, to calibrated light sources – laboratory-calibrated lamps (Stebbins & Kron 1957; Hayes 1970) or blackbody sources setup in situ (Oke & Schild 1970; Tüg et al. 1977) – placed at a distance. Another calibration effort was based on using theoretical models of stellar spectral energy distributions (SEDs), e.g. for three hot DA white dwarfs located in the Local Bubble (Bohlin 1996, 2014; Rauch et al. 2013). This provides high internal accuracy, but its absolute color accuracy is difficult to evaluate independently of stellar models. Any error in the model of the color of these standard stars will directly propagate to the flux calibration applied to the SN fluxes. Flux calibrations from both of these systems have been transferred to observations of secondary standard stars. Observations of an extended network of primary and secondary standard stars on the model-based system, known as CALSPEC[1] (Bohlin 2014), provide the calibration of the instruments mounted on HST.

A more recent approach for physical calibration proposes to transfer a high precision detector-based laboratory calibration to a light source used to illuminate a telescope and its attached science instrument (Stubbs & Tonry 2006). Such transfer is achieved by sequentially observing several quasi-monochromatic light sources with a telescope and then comparing the amount of light measured by the instrument with a calibrated detector that continuously monitors the emitted light. At optical wavelengths, NIST-calibrated (National Institute of Standards and Technology) silicon photodiodes are commonly used as the detector. When the calibrated instrument is a spectrograph, the consequent observation of standard stars provides a calibration network independent of the white dwarf models, after measuring and correcting for atmospheric extinction. This can, hence, be easily used by any observing program.

During the past decades several calibration devices were built based on the detector laboratory calibration approach, they mostly differ on aspects concerning their configuration, the light source selected and the instrument to calibrate (ITC) with the telescope system. Such experiments are listed in Table 1 and briefly described below. Common to all projects is the calibration to a primary laboratory standard. All except one project – NISTstars – refer to the Primary Optical Watt Radiometer (POWR), which is operated by NIST. This primary standard relates the optical to electrical power using a monochromatic source, via the optical / electrical heating of a cryogenic light trap. NIST then transfers the flux scale to photodiodes of type Hamamatsu S2281, which are then used by the different projects to calibrate their systems.

Collimated Beam Projector (CBP) for DECam, LSST and Pan-STARSS: For DECam and LSST CBP, the monochromatic light of a tunable laser is used to illuminate an integrating sphere (IS). The homogeneously

[1] `http://www.stsci.edu/hst/observatory/cdbs/calspec.html`

illuminated exit port is used to illuminate a 2D pinhole array. These holes together with collimating optics create a grid of artificial planets which are then observed by the ITC. The flux emitted by the system has been calibrated in the lab against a monitoring photodiode mounted within the IS. The main difference between the DECam CBP (Coughlin et al. 2016) and the LSST CBP (Ingraham et al. 2016) listed in Table 1 is in the type of collimator. The DECam CBP uses a photographic objective as collimator while the LSST CBP uses a fully reflective Schmidt telescope design. In both cases several relative pointings of the CBP and ITC are needed to sample the complete entrance pupil. The Pan-STARSS CBP (Tonry et al. 2012), the second calibration device deployed for Pan-STARSS, uses the monochromatic light of a tunable laser to feed a fiber bundle which illuminates a projection telescope. A calibrated photodiode is placed in the telescope beam to measure the photon flux. The beam is slightly unfocused to cover ∼1/3 of the Pan-STARSS field of view at a time.

DECal & calibration device for Pan-STARSS: A flat field screen, illuminated by monochromatic light, is used to measure the filter curves of the ITC. The flux level emitted by the screen is monitored by a photodiode. As the screen provides diffuse illumination, corrections such as star flats are needed to account for the enhanced scattering within the ITC. The difference between the two projects is the used light source. In DECal (the other calibration device used for calibrating DECam) a monochromator lamp setup is used (Marshall et al. 2013), while in the first calibration device deployed for Pan-STARSS a tunable laser is used (Stubbs et al. 2010). The diffuse illumination covers the complete entrance pupil of the ITC. A prototype of the DECal system was previously deployed at the Swope telescope at Las Campanas Observatory for the calibration of the photometric equipment used in the Carnegie Supernova Project (Stritzinger et al. 2011). For this purpose filter curves were calibrated with a repeatability of ∼ 1%.

NISTstars: An artificial star is created by a broadband light source placed at a distance of > 100 m Deustua et al. (2018). The emitted flux is measured with a spectrograph flux calibrated against a black body light source operated by NIST. The ITC for NISTstars is another spectrograph, which observes this artificial star. A correction has to be applied to the measured flux to account for the atmospheric absorption between the artificial star and the ITC. A direct measurement of the attenuation is performed by using a red HeNe laser. The wavelength dependence is accounted for by atmospheric models. For this project the illumination of the artificial star covers the complete entrance pupil of the ITC.

StarDICE: Similar to NISTstars an artificial star is created by a remote source (Regnault et al. 2016). Here the source is composed of several narrow band Light Emitting Diodes (LEDs). The emitted flux is obtained from careful lab calibrations of the LEDs relative to a NIST photodiode. Further measurements of the ITC throughput are needed (telescope and filter throughput). The atmosphere in between ITC and artificial star is accounted for by modelling and additional information obtained from the atmospheric physics department at Haute-Provence Observatory. The complete entrance pupil of the ITC is covered.

SnDICE: Here a LED light source is placed close to the ITC (Regnault et al. 2015). The geometry of the light source is in between a diffuse source, like a flatfield screen and a collimated beam, like for a distant source. The flux scale of the LED source is carefully calibrated beforehand in the lab and monitored with calibrated photodiodes. For this project several relative pointings of source and ITC are needed.

ACCESS: The Absolute Color Calibration Experiment for Standard Stars (Kaiser et al. 2010) was based on a telescope with imaging and spectroscopic instruments launched by a rocket into a sub-orbital trajectory. Within each flight the telescope was supposed to be for ≈ 400 s at an altitude of more than 100 km. The telescpoe plus instrument were meant to be carefully calibrated before and after each launch via a artificial star source relative to a NIST primary standard. Prior to the launch and while parachuting to the ground an on board calibration device would monitor changes of

Table 1. Past, Current & Future Projects performing instrumental flux calibration

Project name & ref.	Location	Instrument type	Wavelength range in nm	Setup	Light source type
DECam CBP Coughlin et al. (2016)	CTIO (Chile)	imager	400-1000	in-situ, artificial planet	tunable laser
LSST CBP Ingraham et al. (2016)	Cerro Pachon (Chile)	imager	320-1125	in-situ, artificial planet	tunable laser
Pan-STARSS CBP Tonry et al. (2012)	Hawaii (US)	imager	320-1100	in-situ, artificial planet	tunable laser
DECal Marshall et al. (2013)	CTIO (Chile)	imager	300-1100	local, flatfield screen	7 × LEDs, lamp+monochromator
Pan-STARSS Stubbs et al. (2010)	Hawaii (US)	imager	400-1050	local, flatfield screen	tunable laser
NISTstars Deustua et al. (2018)	Mt. Hopkins (Chile)	spectrograph	≈400-1050	Source at large distance	broad band light source
StarDICE Regnault et al. (2016).	OHP (France)	imager	400-1000	Source at large distance	16 × LEDs
SnDICE Regnault et al. (2015)	CFHT Maunakea (US)	MegaCam imager imager	300-1000	in-situ, artificial planet	LED without Collimator
ACCESS Kaiser et al. (2010)	space	spectrograph imager	350-1700	lab calibration unit before and after flight	lamp+monochromator
Altair Albert (2011)	high altitude balloon	imager or. spectrograph	440, 532, 639, 808	source above atmosphere	4 × laser diodes
ORCASat Albert et al.	LEO satellite	imager or. spectrograph	440, 532, 639, 808	source in orbit	4 × laser diodes
ORCAS Peretz et al.	HEO or L2 satellite	imager or. spectrograph	TBD	source in orbit	8–14 × laser diodes
SCALA CBP Lombardo et al. (2017)	UH88 Maunakea (US)	Integral Field Spectrograph	300-1000	in-situ, artificial planet	lamp+monochromator

the instrument. For this purpose the on board calibration was planned to use flux stabilized LEDs to illuminate the instruments via diffuse reflection off a screen mounted in the telescope cover. The mission, currently stopped, was designed to provide calibrations for Vega and Sirius as well as other standard stars between 6th and 10th magnitude.

Altair & ORCASat & ORCAS: A high altitude balloon or small satellite (respectively) carries an IS illuminated by laser diodes. The emitted flux is measured via a local NIST photodiode (Albert 2011) . As the source is at large distances from the ITC, which is on the ground, the source looks like an artificial star and illuminates the complete entrance pupil. The balloon continuously sends its position to the ground, so that the ITC can track the artificial star. In this case, the ITC calibration includes also the atmospheric absorption, as the balloon / satellite is high enough in the atmosphere. The orbits planned for the satellites ORCAS and ORCASat are different: ORCAsat is in a low earth orbit, which makes it move in the sky too fast for most telescopes on the ground to track it. ORCAS (Peretz et al. 2019) will have a high elliptical Earth orbit or an L2 halo orbit such that ORCAS will move very slowly on the sky, such that it can be tracked by the ITC.

Each solution from this list has its advantages and disadvantages, e.g., the calibration devices placed at large distances from the ITC suffer less from stray light created within the calibration device itself, as the beam is collimated and is, therefore, similar to the celestial observation. However, these ground-based devices need to take into account the atmosphere between ITC and calibration device which is not negligible and adds to the final systematic calibration error.

We find imaging devices as well as spectrographic devices among the project ITCs. In the case the standard stars are calibrated using spectrographs (so spectroradiometrically), the calibration is corrected for instrumental and atmospherical artifacts and can be used by everyone. In the case of imaging systems, the calibration incorporates integration over the instrument passband (the passband here includes atmospheric transmission as well as the instrumental transmissions, filter curves and detector sensitivities). To use these calibrations at other instruments requires the precise knowledge of the wavelength dependence of each component.

In this paper we describe the first results of the SNIFS Calibration Apparatus SCALA, our contribution to this general effort. SCALA, previously described in Lombardo et al. (2017), Küsters et al. (2016), Lombardo et al. (2014), builds on the past experience, described above, and provides an alternative approach. SCALA is an in-situ flux-calibration device developed for the SuperNova Integral Field Spectrograph (SNIFS, Lantz et al. 2003), mounted on the University of Hawaii 2.2 m telescope (UH88) on Maunakea. SCALA is aimed at calibrating the instrumental response of the "telescope + SNIFS" system to <1% precision. The advantage in calibrating SNIFS with such precision is that it is an integral field spectrograph, thus allowing us to produce spectrophotometric calibrated spectra of standard stars. Additionally the high elevation of Maunakea, provides less overall atmospheric extinction, low absorption due to atmospheric water, and the existence of a well-defined inversion layer that further suppressed extinction from aerosols – the most time-variable broadband atmospheric extinction component. These effects are accounted for and corrected nightly from standard stars observations (Buton et al. 2013). Therefore, the resulting physical calibration can be directly transferred to standard stars. These can then be used in a completely general fashion by any telescope, whether in space or on the ground.

In this paper we discuss the concept and design of SCALA (Section 2), and the data obtained using its calibrated photodiodes (Section 3). In Section 4 we discuss in detail the key pre-commissioning and post-commissioning tests conducted to measure the performance and stability of the system. The second post-commissioning run additionally commissioned an aperture mask. We explain the calibration methodology that was imple-

mented, and show the first throughput measurements in Section 5 and 6. The origins of, and limits on, potential sources of systematic uncertainty are discussed in Section 7. Some of the SCALA systematic uncertainties have already been described in detail in Küsters et al. (2016), hereafter K16.

2. SCALA concept

SCALA (Figure 1) is meant to provide a better than 1% precision relative flux calibration (the type of calibration that mostly impact SN Ia cosmology) of the "telescope + instrument" system response, in such a way that this system can then be used to refine the standard star network. SCALA is an in-situ flux-calibration device designed to produce a uniform illumination of the focal plane, i.e., a flat-field, while monitoring the light emitted using a calibrated photodiode. In the following subsections we will briefly describe SNIFS and then we will focus on the design of the calibration device.

Fig. 1. SCALA attached at the ladder of the dome of the UH88 telescope. The projector modules with the three mirrors and the IS hold in front of them are visible in the image, below SCALA is located the lamp+monochromator system and the electronics boxes.

2.1. SNIFS

The SuperNova Integral Field Spectrograph (IFS) SNIFS (Lantz et al. 2003), located at the bent Cassegrain port of the UH88 on the summit of Maunakea, is composed of three channels: two spectroscopic (blue and red, respectively) and one imaging. Each spectrograph camera holds a E2V 2k×4k CCD. The dual-channel spectrograph simultaneously covers 3200–5200 Å (*B*-channel) and 5100–10 000 Å (*R*-channel) with line spread functions having FWHM values of 5.23 Å and 7.23 Å, respectively. The spectrograph samples a 6.4" × 6.4" field-of-view through a combination of a microlens array made of 15×15 lenses followed by a collimator, a grism and a camera. Each of the 225 0.43" × 0.43" spatial elements of the microlens arrays that segment the focal plane and are subsequently dispersed is called a spaxel.

The imaging channel has a $9.4' \times 9.4'$ field-of-view, covered by two $2k \times 4k$ E2V CCDs. It is equipped with a filter wheel composed of *ugriz* (SDSS) filters, a pinhole grid and a multiple-band filter. In regular SNIFS observations, the filter wheel is set on the multiple-band filter and the images are used for guiding and relative flux calibration during non-photometric nights (Da Silva Pereira 2008). The multiple-band filter produces observations of different areas of the sky in distinct bands. We use the imaging channel for aligning the telescope with SCALA and for testing potential sources of systematic uncertainty in the SCALA system (more details are presented in Lombardo et al. (2017)).

SNIFS data reduction was summarized by Aldering et al. (2006) and updated in Section 2.1 of Scalzo et al. (2010). The flux calibration was developed in Section 2.2 of Pereira et al. (2013), based on the atmospheric extinction derived in Buton et al. (2013). The SNIFS data used in this paper are reduced according to the initial steps of the SNIFS pipeline, e.g. bias removal and wavelength calibration, but then stopping the pipeline reduction before flat fielding and flux calibration. By processing our data in this way we can reduce

the possible systematic difference between the processing of calibration and science frames.

2.2. SCALA design

SCALA (Figure 1) consists of 18 f /4 (i.e. focal length of 80 cm) parabolic mirrors with diameters of 20 cm each, distributed over the entrance pupil in a nearly hexagonal arrangement. Integrating spheres fed by a wavelength-tunable light source (from UV to IR) illuminate the mirrors producing 18 collimated beams with opening angles of 1°, thereby forming a uniform "planet" rather than a star. To monitor the stability of the light source, as well as the flux produced by the device, two Cooled Large Area Photodiodes (CLAPs) are installed in front of two of the 18 mirrors, in such a way that they can measure part of the reflected light. These photodiodes are the flux standards meant to transfer NIST calibration to the light source (SCALA light-beams).

The lamp system of SCALA is composed of an APEX-Illuminator with a 150 W Xe lamp, for the wavelength range 3300-7020 Å, and a halogen lamp used between 7020 Å and 10000 Å. These lamps illuminate a monochromator (Cornerstone 260, Newport) used in the configuration with two gratings, of 1200 l/mm and blaze wavelength of 3500 Å and 7500 Å respectively. The two gratings are selected separately depending on the wavelengths range to calibrate. The line spread function of SCALA is set by the dimensions of the entrance and exit slits of the monochromator and it has a FWHM of 35 Å, which provides a good balance between spectral resolution and light level. The lamp system is also equipped with order sorting filters, with cut-on at 3090 Å (F1) and at 4950 Å (F2), to prevent the light, that will be dispersed as second order, from entering the monochromator. Weak second order light starts appearing from 9000 Å and stays subdominant until 9700 Å. We conservatively limit our calibration range up to 9000 Å. A double monochromator is planned as upgrade to the SCALA device in order to reduce these types of systematic effects as well as stray light from the monochromator (Küsters et al., in prep.). In Table 2 the different configurations of lamps, gratings and filters, used in the wavelength range during regular calibration, are shown. For gratings and filters the value reported are the blaze and cut-on wavelengths respectively.

Table 2. Configurations of lamps, gratings and filters, used when operating SCALA for different wavelength ranges.

Wavelength Range [Å]	Lamp	Grating blaze [Å]	Filter cut-on [Å]
3200 – 4500	Xe	3500	none
4500 – 5220	Xe	3500	3090 (F1)
5220 – 6240	Xe	7500	3090 (F1)
6240 – 7020	Xe	7500	4950 (F2)
7020 – 10000	halogen	7500	4950 (F2)

A Ceramoptec (Optran WF1) fiber bundle brings the light from the monochromator to the six integrating spheres (ISs), by splitting into six different arms. The fibers inside these arms are composed in such a way that each arm has 33 fibers distributed across the exit slit of the monochromator to guarantee a homogeneous sampling of the entire slit. Each IS of SCALA has three exit holes which in turn illuminate the three mirrors that are placed in front of them, forming a projector module (1 IS + 3 mirrors). A projector module, hence, generates three uniform and collimated beams, as detailed in Lombardo et al. (2017), based on the concept developed by Vaz (2011)[2]. The six projector modules together, then, generate the final illumination of the UH88 telescope, by covering 17% of the primary mirror. We designed a mask which has to be mounted at the top of the telescope to cover the non-illuminated regions. With the mask mounted, the standard stars observed illuminate the same region of the primary mirror calibrated with SCALA. Note that the mask is only necessary when recalibrating standard stars – wavelength-relative throughput measurements can be made without it.

[2] http://hdl.handle.net/1721.1/65435

3. The laboratory-reference system

The reference system continuously monitors the light produced by SCALA. For this task we use two CLAPs (Cooled Large Area Photodiode), which were, in turn, directly calibrated to photodiodes calibrated by NIST. The two CLAPs have been produced by the DICE team (Regnault et al. 2015) and also have been used by their calibration experiments, SnDICE and SkyDICE. These photodiodes (Hamamatsu S3477-04) are very stable and highly sensitive (0.5 A/W at 9600 Å). Their calibration precision is 0.7% or better in the wavelength range of interest. They have a sensitive area of $5.8 \times 5.8\,\mathrm{mm}^2$ and are equipped with a two-stage Peltier cooler, which keeps them at a temperature of $-14\,^{\circ}\mathrm{C}$. These devices are small and compact enough to be held by a U-shaped structure that is mounted in front of our beams without obscuring the light from the integrating sphere. This structure allows their installation in front of any SCALA projection mirror. During operations, one photodiode is used to continuously monitor the light emitted by SCALA. The second photodiode is used for calibration and as a redundant monitoring system.

The data obtained from the photodiodes include three measurements for each wavelength scanned during the telescope calibration procedure: before and after the light exposure we expose the photodiodes for about 2 s with the monochromator's shutter closed to measure the background level, and between these we perform the light exposure of variable lenght with the monochromator's shutter opened. The photodiodes continuously measure with a frequency set at 1 kHz during these three phases (Figure 2). The two background exposures, performed with the monochromator shutter closed, track the dark current of the photodiode and the background ambient light, and their potential time variation. The dark current that the photodiode experienced during the light exposure can hence be measured and subtracted, by averaging these two background exposure, achieving a random error < 0.2% for calibration of most wavelengths for nighttime photodiode data.

The element ultimately setting the exposure time for the SCALA wavelength observation is, therefore, the shutter of the monochromator. CLAP data are thus not only used as light monitor, but also as an independent mean to measure the exposure time, with a precision better then < 0.01% for our shortest exposure times.

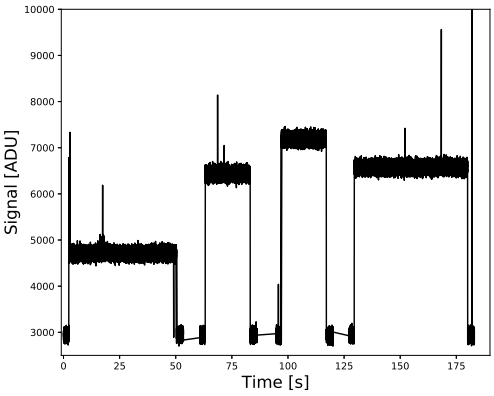

Fig. 2. Example of the data obtained from one CLAP for a SNIFS blue-channel exposure. Notice the different exposure time for each wavelength, depending on the light level and SNIFS transmission, and also the presence of $\sim$ 2 s background exposures before and after observing each wavelength. The outliers in the data are cosmic rays, which are subsequently removed by the analysis software.

4. SCALA relative light output characterization

A precise flux calibration of the "telescope + SNIFS" system can be obtained only after performing a precise characterization of the calibration device itself. We divided this process in two steps: 1) measurements in the lab of the response as function of wavelengths of each SCALA component, 2) measurements of the fully integrated system in-situ. Consistency between the two approaches will verify that the

SCALA output and monitoring is understood at the component level.

Laboratory measurements Relative color response measurements of the individual SCALA components (six ISs, six fiber bundle arms and 18 mirrors) were performed in the lab with specific test benches. Each response curve was measured at the same time as a fixed reference, in such a way that systematics effects due to, e.g., temporal variation of the light system, would not affect the final results. For more information on the different set-ups and strategies adopted for this characterization phase, please refer to Lombardo et al. (2017).

The single color responses were then numerically combined to mimic the fully integrated system by calculating the quantity:

$$P_{i,j,k}(\lambda) = \tau_{f_i}(\lambda) \cdot \tau_{IS_j}(\lambda) \cdot \tau_{m_k}(\lambda) \quad (1)$$

where $P_{i,j,k}(\lambda)$ is the relative response of one of the SCALA beams when using the i-th fiber bundle, j-th integrating sphere and k-th mirror, all taken with respect to the reference beam. The sum over all 18 beams is used as an estimate of the total light expected to be produced by SCALA.

Commmissioning in-situ measurements During the two commissioning phases in 2014 and 2015 we measured the SCALA beam transmissions again, but now using the fully assembled and mounted set-up. We held the reference CLAP photodiode stationary, to always monitor the same SCALA beam, and then moved the other CLAP sequentially to the 17 remaining beams. For each one of these we observed a series of monochromatic lines, thereby obtaining the relative wavelength response of the 17 beams with respect to the reference beam. The normalized sum over these relative measurements provides the color of the SCALA light that illuminates SNIFS.

We express the wavelength dependence of the SCALA light output, E_s, as follows:

$$E_s(\lambda_c) = 1 + \sum_{i=n=2}^{18} \frac{C_t^{i(n)}(\lambda_c) \cdot D_t(\lambda_c)}{C_r^n(\lambda_c) \cdot D_r(\lambda_c)}, \quad (2)$$

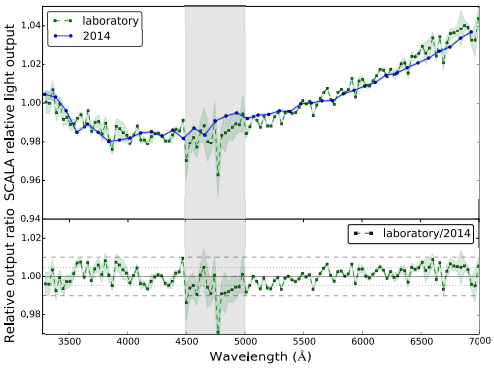

Fig. 3. The quantity E_s is shown in the top panel. In green is the wavelength dependence of the SCALA relative light output estimated from the laboratory measurements. In blue is that measured from the commissioning in May 2014. Both have been normalized with respect to their average to compare their color trend. The bottom panel shows the ratio between the laboratory measurement and the 2014 commissioning measurements. The dashed lines represent the ±1% range around the averaged ratio of 1.000 (full line). The dotted lines are the measured standard deviation of 0.4%. The vertical gray band delimits the region where weak emission lines of the Xe lamp are located (4500-5000 Å). The measurements have been performed with the Xe lamp and therefore they only go up to 7000 Å. (Lombardo et al. 2017)

where C_r^n is the n-th flux measurement by the reference CLAP corresponding to the flux, C_t^i, measured by the test CLAP in the i-th beam for the SCALA line centered at λ_c. D_r and D_t are the factors to convert the reference CLAP and the other CLAP measurements, respectively, from ADU to W, obtained by weighting the photodiode calibration curve – provided by the DICE team – by the SCALA line profile. E_s is therefore the number of times the light measured by the reference CLAP should be multiplied to represent the total SCALA output. If all beams were identical to the reference beam, E_s would be equal to 18 for every wavelength.

The comparison between these three measurements of the total SCALA color re-

sponse (summed over the 18 beams) are shown in Figure 3 for the lab (computed from Equation 1) vs 2014 commissioning and in Figure 4 for the two commissioning in 2014 and 2015 (computed as in Equation 2). The responses of ISs, mirrors and fiber bundles measured in the lab are each scaled by the respective IS, mirror or fiber bundle response of the reference beam, thus mimicking the in-situ setup wherein responses are measured relative to the reference CLAP. The sums over these 18 response is shown in Figure 3 and it is compared to the commissioning measurement in 2014. The measurements have been normalized to their average values since we are only interested in comparing their color trend and not their absolute values. These averages are computed on the wavelength range shown in the plot and are 19.12 and 18.95 for the lab and 2014 curves respectively (this offset is within the errors).

As can be seen in Figure 3 (bottom panel) the component-wise measurements and the in-situ in 2014 match well within the errors (shadowed area around the line), for the entire wavelength range measured, showing a scatter of 0.4%. The agreement of the curves, together with the consideration that they have been measured with independent setups, demonstrates the success of our method and that we are able to reconstruct the wavelength behavior of the SCALA light output with a precision better then 1%, by monitoring only two of the SCALA beams at a time.

An evolution of the system response on longer time scales has been observed when comparing the two in-situ commissioning measurements. In Figure 4 a difference is apparent at bluer wavelengths between the 2014 and 2015 data. These curves (left and right panels) are normalized with respect to their average values of 20.09 and 19.46 for the 2014 and 2015 measurements respectively, computed over the full wavelength range. One known difference was that the SCALA mirrors were cleaned before performing the measurements in 2015. The reference mirror was cleaned more thoroughly with respect to the others, due to easier accessibility. Hence, a relative difference between the different beams and the reference beam is expected. From 4700 Å the two curves match again with a scatter of 0.5%.

The variation in the trend at the bluer wavelength end could be due to a more accentuated degradation of the reference beam with respect to the others. More specifically, a comparison between the responses of the beams belonging to the same IS as the reference beam do not show a deviation in the blue end, excluding a different degradation of CLAP1 with respect to CLAP0. Instead a color trend appears when the other beams are included in the comparison. This suggests that we measure an evolution of the reference IS and/or fiber bundle arm with respect to the others. One of the beams illuminated by the same IS as the reference beam is plotted in Figure 4 with black circles with the name "single beam 2015", normalized with its average value of 0.70. Its wavelength trend is mostly smooth and achromatic, suggesting that the two CLAPs did not degraded differently.

We thus conclude that we understand how the SCALA components combine to the full system. We also find that the relative system throughput can change on longer time-scales, and that E_s should be remeasured in connection with any extensive calibration campaign.

5. Calibration strategy

We turn now to the description of the strategy adopted to use SCALA to calibrate the "telescope + SNIFS" system.

5.1. SNIFS data

The SCALA passband has a nearly triangular shape with a FWHM of 35 Å. We have verified that selecting a separation of 500 Å between the SCALA wavelengths observed within one SNIFS exposure yields negligible cross talk issues and overlaps between adjacent wavelengths (K16). We also avoid crowded images or long exposures with SNIFS, by limiting the number of wavelengths observed per exposure to 4 for the blue channel calibration (3300 Å - 5000 Å) and to 10 for the red one (5000 Å - 10000 Å).

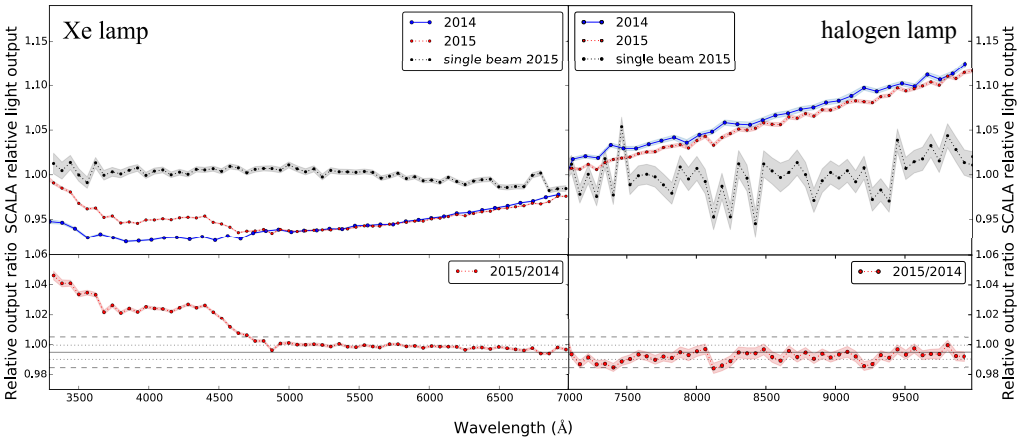

Fig. 4. The quantity E_s is shown in the top panel for both figures, the SCALA relative light output from the commissioning in May 2014 is in blue and the latest commissioning in May 2015 is in red. Both are normalized to their average values to compare only their color trend. One of the mirrors illuminated by the same IS as the reference for the 2015 SCALA relative efficiency measurements, normalized by its average value, is shown using solid black circles. The bottom panels show the ratios between the two sets of commissioning measurements. The dashed lines represent the ±1% range around the averaged value computed for the measurements from 4700 Å to 10000 Å, where a gray offset is present. The full line, around 0.995, is the average and the dotted lines span the standard deviation interval (±0.005). The quantities in the left panel refer to E_s measured with the Xe lamp while the right panel shows the measurements with the halogen lamp. (Lombardo et al. 2017)

A typical SNIFS exposure, after processing as in Section 2.1, is shown in Figure 5 for an observation of SCALA by SNIFS in the blue channel. A SCALA observing sequence that calibrates the full SNIFS wavelengths range with a chosen wavelength sampling (from 30 Å on) therefore consists of multiple SNIFS exposures, each containing four or ten monochromatic lines, depending on the SNIFS channel. The exposure time for each wavelength observation was set such that we obtain a corresponding S/N >100 per spaxel. The overall time required for a complete SNIFS calibration is 8 hrs with typical exposure times from 30s to 180s per wavelength. However, it is also possible to choose a coarser wavelength sampling of 150 Å, to obtain a calibration of SNIFS in less then 2 hours.

5.2. Observation of SCALA

During 2015 we observed in the nights from the 3rd till the 7th of June several standard stars and our calibration device with the newly commissioned entrance pupil mask installed. Dividing the nights in blocks of standard stars and SCALA observations allows to track possible evolution of SNIFS during the night and verify its repeatibility.

The night was subdivided into 5 sections: a ∼2 hr SCALA calibration sequence starting from 3330 Å with steps of 180 Å was performed before twilight, when the influence of ambient light in the dome was already much suppressed, then the dome was opened and regular SNIFS standard star observations were performed for ∼2 hr. Subsequently the dome was closed again and another SCALA calibration sequence was observed with the same steps but starting at 3390 Å this time. After that, standard stars were observed until morn-

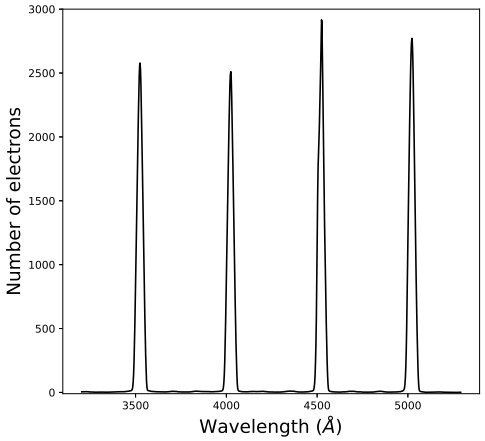

Fig. 5. Example of the wavelength-calibrated spectrum obtained from the average on all the spaxels of SNIFS for the blue channel. This is a typical exposure showing the 500 Å separation between the different wavelengths observed (the same as in Figure 2) and the nearly consistent number of electrons per wavelength due to a careful selection of the SCALA exposure time for each wavelength. The characteristic triangular shape and 35 Å FWHM of the SCALA line profile is also evident. This SNIFS exposure shows the same wavelengths observed by CLAP in Figure 2.

ing twilight, after which a final SCALA calibration sequence starting from 3450 Å was made. Adding together all the SCALA calibration sequences performed during the night we obtain a complete SNIFS calibration sampled with 60 Å steps, which translates into 111 measurements on the "telescope + SNIFS" instrumental response. Furthermore, to ascertain the stability of the "telescope + SNIFS" system during the night, we repeated the observations of a set of SCALA lines during each sequence. The comparison between these repeated observations is discussed in the systematic section.

6. Throughput measurements and other uses

The ultimate goal for SCALA is to provide precise measurements of the "telescope + SNIFS" system throughput. The throughput measurement is accomplished by comparing the observations of SCALA made by SNIFS, with the reference light recorded by the CLAP according to:

$$T(\lambda_c, \mathrm{spx}) = \frac{\int I_{\mathrm{SNIFS}}(\lambda, \mathrm{spx}) E'(\lambda) d\lambda}{C_r(\lambda_c) \cdot D_r(\lambda_c)} \cdot \frac{G}{E_s(\lambda_c)} \quad (3)$$

where $I_{\mathrm{SNIFS}}(\lambda, \mathrm{spx})$ is the SCALA line intensity centered at λ_c observed by SNIFS in each spaxel, spx, in electrons and $E'(\lambda)$ is the energy of the photon for the wavelength λ; C_r is the integrated light measured by the reference CLAP (over the SCALA line exposure time); D_r is the factor to convert the reference CLAP measurement from ADU to W, as in Equation 2; $E_s(\lambda_c)$ is the SCALA light output relative to the reference CLAP from the 2015 measurements as in Equation 2 and shown in Figure 4 (without normalization this time); G is the geometrical factor that accounts for the different dimensions of the CLAP and SNIFS and also their different fields of view. The geometrical factor, G, is determined by multiplying the ratio of areas of the CLAP (5.8×5.8 mm) versus area of a SCALA mirror against the ratio of the solid angles of the SCALA beam (1°) versus that of a SNIFS spaxel.

By averaging the throughput measurements over all spaxels in SNIFS, we obtain the mean throughput shown in Figure 6. This curve combines the data from the three blocks of SCALA-calibration-sequences. Once the SCALA throughput datacube has been built it can be directly applied to the standard stars datacube generated by the SNIFS pipeline, thus providing newly calibrated standard star spectra.

There are several additional possible applications for SCALA: it can be used to directly quantify the zero- and second-order light in the spectrograph for estimating whether it contaminates the first-order light, to perform a stray light study in the telescope optics, to measure cross-talk between spaxels by observ-

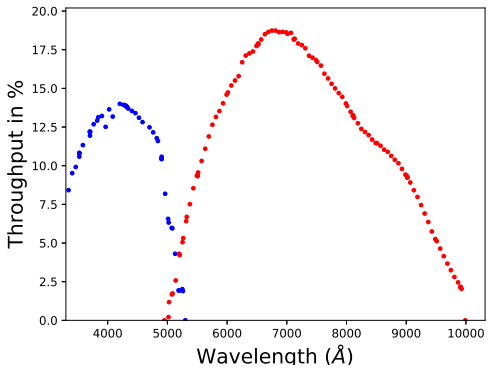

Fig. 6. The nighttime throughput, $T_{\lambda_i,spx}$, of the telescope plus SNIFS, averaged over all SNIFS spaxels. The blue and red circles represent the throughput measured by illuminating the blue and red spectroscopic channels, respectively, and the telescope with SCALA. The data include all measured wavelengths and extends above 9000 Å, the maximum wavelength considered in this paper for calibration.

ing individual SCALA wavelength exposures, to obtain the filter+CCD curves for the SNIFS imaging channel filter set.

We have also tested performing SNIFS throughput measurements with reduced exposure times, and during daytime. These changes would allow daily determinations of the telescope+SNIFS throughput. Even though, in this case, the statistical precision would be lower than usual and there might be some ambient light contamination, the overall result still showed a smooth, high-precision measurement.

Therefore, SCALA can also be used for fast estimation of throughput changes, e.g., before and after cleaning of the optics, or filter replacement. Moreover, due to the 1° angular extent of the SCALA calibration beam as seen at the focal plane of the telescope, such a device can also be used by other instruments mounted at the telescope having wide fields of view.

7. Systematic errors

In this section we carefully examine the various sources of uncertainty. The known or potential sources of systematic uncertainty are summarized in Table 3. Some of these errors are correlated, thus, the net systematic uncertainty will be much less than the quadrature sum of the values listed in Table 3. The final error, will be presented by Küsters et al. (in prep).

Our calibration precision can only aim at being as good as the reference system used: the CLAPs are calibrated by the DICE team (Regnault et al. 2015) and have uncertainties – mostly dominated by the NIST photodiode calibration uncertainties – around 0.74% between 3200 and 3400 Å, then < 0.32% up to 4700 Å and <0.18% above 4700 Å. In this we have assumed that the 2σ uncertainties quoted by NIST are Gaussian, so we can convert them into 1σ uncertainties.

From the elements composing Equation 3, the biggest contribution to the error is due to the E_s term. This particular set of measurements has been performed in rather different conditions than the usual ones, making it subject to several sources of contamination: they can have residual ambient light contamination not properly corrected by the CLAPs background measurements (they were measured during daytime), and finally, wavelength uncertainty caused by the monochromator reproducibility (as these lack associated SNIFS observations to provide precise wavelength measurements) and reproducibility of the photodiode position for each mirror when cross-calibrating each beam will add to their final total error.

7.1. Systematic errors in the E_s term

Ambient light contamination For these daytime measurements there are two cases that can occur: diffuse and scattered ambient light that smoothly drifts with time, and scattered ambient light that quickly varies on a time scale of seconds, probably modulated by clouds crossing the sky. The former case, appearing on time-scales longer than individual

SCALA line exposures, can be accurately accounted for using the CLAP background measurements and constrained to an error <0.4%. In K16 we confirm that most ambient light variations are slow, but that occasional faster modes exist, e.g., due to clouds. Such fast variations, with non-optimal background removal, are all found to be strongly correlated between the two CLAPs. Thus, taking this correlation into account we found that the total error on E_s (which is a ratio between data from the two CLAPs) can be constrained to 0.5%. Ambient light is not a concern during nighttime measurements, where CLAP dark current variations can be reconstructed to better than 0.2% of the faintest (longest exposure) line emitted by SCALA.

Wavelength uncertainty on SCALA relative output SCALA produces monochromatic light through a monochromator and for the SNIFS system throughput estimation we use the wavelength calibration from SNIFS data to evaluate the central wavelengths observed. The monochromator wavelength uncertainty is, however, present in the determination of the SCALA relative output E_s since these measurements are not accompanied by SNIFS exposures. We used the SNIFS wavelengths calibration to verify the stated wavelength precision, by comparing the central SCALA wavelengths estimated from a set of SNIFS exposures with the ones requested to the monochromator. They follow a linear trend, that can be fitted for the blue and red wavelength. The residuals of such fits, after the subtraction of a 20-point running average, show standard deviations of 1.51 Å and 1.01 Å for the blue and red channels, respectively. When recomputing E_s using a wavelength that is artificially increased (or decreased) by one such standard deviation, we find the same result within 0.021% (in the worst case).

Reproducibility of the SCALA relative output We have tested the reproducibility of the SCALA relative output in 2015, by repeating the measurement of one of the 18 SCALA beams after four days of operations. The mean reproducibility is excellent, having a mean of 0.999 and a standard deviation of 0.008. The ratio between the two sets of measurements shows a 0.8% difference for blue wavelengths (< 4700 Å), likely due to a change in the system on time scales of a few days. Relative evolution of the IS and/or fiber bundle arm belonging to the reference projector module with respect to the other SCALA modules, as mentioned in Section 4, is a possible cause. As each beam ratio has a similar amplitude, the final error, after combining all beams, is 0.7% for wavelengths < 4700 Å.

7.2. Other possible systematics in "telescope + SNIFS" system calibration

As the SCALA beams have different relative color efficiencies, they will weight the reflectivity of the corresponding regions of the primary mirror differently. To estimate the potential size of such an effect might have, we use twilight sky images taken with the pinhole array in the SNIFS imaging channel. We mask the full-aperture pupil image in such a way so as to reproduce the SCALA illumination pattern. Then we 1) use the single SCALA beam responses to scale the corresponding beam patterns and sum over the full pupil image, 2) we take again the initial pupil masked image and sum over the pupil image and then scale it for the E_s. The ratio between these two quantities provides the systematic error due to the non-uniform illumination of the entrance pupil of the telescope generated by SCALA and turns out to be < 0.09%.

Another important factor to consider for systematic error concerns the stray light by the SCALA illumination within the telescope. The well-collimated beams of SCALA are designed to minimize the amount of scattered light. However, the beam aperture is still 1°, so rays far off axis might be a source of stray light within the telescope or SNIFS. To study this question we mounted smaller apertures in the IS output ports, thus reducing the SCALA angular extent to half its original size. We observed a set of monochromatic SCALA

Table 3. List of systematic uncertainties that contribute to the total uncertainty on the throughput measurements.

Systematics	σ_T/T
Ambient light in SCALA relative output (daytime clouds)	$< 0.5\%$
Ambient light in SCALA relative output (daytime clear)	$< 0.4\%$
Ambient light in nighttime CLAP data	$< 0.2\%$
Wavelength uncertainty on SCALA relative output	$< 0.021\%$
SCALA relative output stability	$< 0.7\%$ for $\lambda < 4700$ Å $< 0.02\%$ for $\lambda \geq 4700$ Å
Inhomogeneous color illumination of the entrance pupil	$< 0.09\%$
Stray light in 0.5° beam	$< 0.51\%$
CLAP integration over time error	$< 0.07\%$
Optical cross talk in SCALA	$< 0.05\%$
Optical cross talk in SNIFS	$< 0.1\%$
SCALA and SNIFS reproducibility	0.3% for $\lambda \geq 4000$ Å 2% for $\lambda < 4000$ Å
CLAP calibration	0.74% for $\lambda < 3400$ Å 0.32% for $3400 < \lambda < 4700$ Å 0.18% for $\lambda \geq 4700$ Å

lines with and without beam reducers using the spectroscopic channels of SNIFS. The ratios between these measurements show a mean ratio offset from 1, thus confirming finding some amount of scattered ligh. However, any wavelength dependency to the scattered light is small (well below 1%). A linear fit from blue to red wavelengths has range of ±0.51% over the wavelength range of interest, with a borderline significance of $2.9\,\sigma$. There are ongoing tests and SCALA system upgrades (Küsters et al., in prep.) planned to verify and reduce potential stray light observed by the CLAPs themselves and not by SNIFS, due to their different field of views. This situation might cause an important bias in the "telescope+SNIFS" system calibration.

Optical cross talk for SCALA observations is another possible cause of systematics. There are two possible sources of cross-talk: the photodiode might receive scattered light from other beams, or ,in the SNIFS datacube part of the light belonging to one spaxel might be collected in another spaxel, and, because of the geometry of SNIFS optics, such light would be displayed in other wavelengths. In the second case the effect is negligible, since the light from another spaxel is <0.1% of the light integrated in the monochromatic line K16. The cross talk due to scattered light from another beam hitting the calibrated photodiode has been already described in K16 and turns out to be <0.05%.

We also tested the "telescope+SNIFS" system stability through the night, as the throughput measurements were performed by putting together blocks of observations of SCALA performed in between standard stars observation during the night (Section 5). For each of the three SCALA observing block sequences during June 7, 2015, we observed a set of lines in common and we estimated the throughput values associated with them (according to Equation 3). The comparison of these values (the ratio between one against the other two) was centered around 1.001 with standard deviation of 0.3% in the 4000-9000 Å wavelength range. In the 3300-4000 Å region we find a 2% offset for the last SCALA sequence. The origin of this difference is unknown. Repeated observations of this wavelength region may be able to reduce the net calibration error. But for now we take the full amplitude of the offset as a systematic uncertainty. Above 4000 Å the reproducibility of our system is very good and is not a limitation.

8. Conclusion

The description and first results obtained with the SNIFS Calibration Apparatus, SCALA, were summarized in this paper and fully shown in Lombardo et al. (2017). SCALA is built as part of a Nearby Supernova Factory effort to reach a better than 1% color-calibration with the SuperNova Integral Field Spectrograph (SNIFS). It belongs to a global effort in astrophysics that has tried to link the telescope+instrument calibration to laboratory flux standards. Such devices are necessary to improve the cosmological constraints from observations of SNe Ia, since systematic uncertainties on calibration are soon limiting factors when comparing SN Ia distances. SCALA generates 18 beams, which are collimated at the 1° scale and illuminate the focal plane of the telescope uniformly. The SCALA light source system, lamp+monochromator, produces monochromatic light with a triangular line profile and a FWHM of 35 Å.

The flux calibration of a NIST photodiode has been transferred to two photodiodes used as reference system (Cooled Large Area Photodiodes, CLAPs). SCALA is meant to transfer the NIST flux calibration to the UH 88+SNIFS system, and use this calibrated system to determine a NIST-traceable flux calibration of the standard star network. As SNIFS is an Integral Field Spectrograph, a SNIFS recalibrated standard star spectra could be used by any other astronomical observer.

All the color responses of the SCALA components (6 ISs, 6 fiber bundles and 18 mirrors) were singularly characterized in the lab. Their integration into the final in-situ system results in the transmissions of each SCALA beam. During commissioning we again measured the transmission of the SCALA beams, in the fully deployed set-up. The normalized sum over these measurements provides the color of the SCALA light output that illuminates SNIFS. Comparing this quantity with the independent component-wise measurements, we showed that we can reproduce the color trend of the total light generated by SCALA at a level better than 1%. By repeating the in-situ measurements after one year, we saw that both commissioning measurements, from 2014 and 2015, agree very well for wavelengths above 4700 Å, but disagree at bluer wavelengths, hinting at a color evolution of the system. It is therefore essential to repeat the 18 beams characterization before recalibrating the standard stars – the ultimate goal for SCALA.

In the 2015 commissioning, we mixed observations of standard stars with observations of SCALA, from which we calibrated the "SNIFS+UH 88" system with a sampling of 60 Å. During the same night we performed three SCALA calibration sequences (at twilight, middle of the night and after sunrise), and standard stars in the remaining available time slots. By combining these three SCALA observations, we produced a throughput curve of the "SNIFS+UH 88" system. We also give upper limits to the main systematics affecting our measurements, which are all $< 0.7\%$ over the wavelength range of interest (4000-9000 Å).

One of the factors, that still needs to be verified, is the out-of-band emission from the monochromator, which could lead to contamination larger than 1-2%. This scattered light would be observed by the reference photodiode and integrated over its range of sensitivity, while the spectrograph would disperse the light over its spectral range, yielding to a negligible contamination in SNIFS (a 0.05% contamination from an entire line). Future work on SCALA and its upgrades will have to measure and reduce this effect before applying the final calibration on the standard star observations.

The standard star observations taken along with SCALA (Section 5.2) will be presented in Kuesters et al., in prep. Also, a number of upgrades to SCALA are underway which should enable calibration at the sub-percent level. Once the fundamental flux calibration is accurately established, and spectroscopic or imaging instrument will benefit by observing these improved standard stars.

Acknowledgements. We are grateful to Kyan Schahmaneche, Laurent Le Guillou and Nicolas Regnault from LPNHE for providing the CLAP modules and support. We thank the technical staff of the University of Hawaii 2.2 m telescope. We recognize the significant cultural role of Maunakea within the indigenous Hawaiian community, and we

appreciate the opportunity to conduct observations from this revered site. This work was supported in part by the Director, Office of Science, Office of High Energy Physics of the U.S. Department of Energy under Contract No. DE-AC02-05CH11231. Support in France was provided by CNRS/IN2P3, CNRS/INSU, and PNC; LPNHE acknowledges support from LABEX ILP, supported by French state funds managed by the ANR within the Investissements d'Avenir programme under reference ANR-11-IDEX-0004-02. Support in Germany was provided by the German Science Foundation through TRR33 "The Dark Universe" as well as through the graduate school "Mass, Spectrum, Symmetry" GRK1504 of the Humboldt University Berlin, the Technical University Dresden and DESY Zeuthen. In China support was provided from Tsinghua University 985 grant and NSFC grant No 11173017. Some results were obtained using resources and support from the National Energy Research Scientific Computing Center, supported by the Director, Office of Science, Office of Advanced Scientific Computing Research of the U.S. Department of Energy under Contract No. DE-AC02- 05CH11231. We thank the Gordon & Betty Moore Foundation for their continuing support.

References

Albert, J. 2011, The Astronomical Journal, 143, 8

Aldering, G., Antilogus, P., Bailey, S., et al. 2006, ApJ, 650, 510

Betoule, M., Kessler, R., Guy, J., et al. 2014, A&A, 568, A22

Betoule, M., Marriner, J., Regnault, N., et al. 2013, A&A, 552, A124

Bohlin, R. C. 1996, AJ, 111, 1743

Bohlin, R. C. 2014, AJ, 147, 127

Buton, C., Copin, Y., Aldering, G., et al. 2013, A&A, 549, A8

Coughlin, M., Abbott, T. M. C., Brannon, K., et al. 2016, in Proc. SPIE, Vol. 9910, Society of Photo-Optical Instrumentation Engineers (SPIE) Conference Series, 99100V

Da Silva Pereira, R. 2008, Theses, Université Paris-Diderot - Paris VII

Deustua, S., Woodward, J. T., Rice, J. P., et al. 2018, in American Astronomical Society Meeting Abstracts# 231, Vol. 231

Hayes, D. S. 1970, ApJ, 159, 165

Ingraham, P., Stubbs, C. W., Claver, C., et al. 2016, in Ground-based and Airborne Telescopes VI, Vol. 9906, International Society for Optics and Photonics, 99060O

Kaiser, M. E., Kruk, J. W., McCandliss, S. R., et al. 2010, arXiv preprint arXiv:1001.3925

Küsters, D., Lombardo, S., Kowalski, M., et al. 2016, in Society of Photo-Optical Instrumentation Engineers (SPIE) Conference Series, Vol. 9908, Ground-based and Airborne Instrumentation for Astronomy VI, ed. C. J. Evans, L. Simard, & H. Takami, 99084V

Lantz, B., Aldering, G., Antilogus, P., et al. 2003, in SPIE Proceedings Series, Vol. 5249, 146–155

Lombardo, S., Aldering, G., Hoffmann, A., et al. 2014, in Society of Photo-Optical Instrumentation Engineers (SPIE) Conference Series, Vol. 9147, Ground-based and Airborne Instrumentation for Astronomy V, ed. S. K. Ramsay, I. S. McLean, & H. Takami, 91474R

Lombardo, S., Küsters, D., Kowalski, M., et al. 2017, Astronomy & Astrophysics, 607, A113

Marshall, J., Rheault, J.-P., DePoy, D., et al. 2013, arXiv preprint arXiv:1302.5720

Oke, J. B. & Schild, R. E. 1970, ApJ, 161, 1015

Pereira, R., Thomas, R. C., Aldering, G., et al. 2013, A&A, 554, A27

Peretz, E., Mather, J., Slonaker, R., et al. 2019, in Bulletin of the American Astronomical Society, Vol. 51, 284

Rauch, T., Werner, K., Bohlin, R., & Kruk, J. W. 2013, A&A, 560, A106

Regnault, N., Barrelet, E., Guyonnet, A., et al. 2016, in Astronomical Society of the Pacific Conference Series, Vol. 503, The Science of Calibration, ed. S. Deustua, S. Allam, D. Tucker, & J. A. Smith, 165

Regnault, N., Guyonnet, A., Schahmanèche, K., et al. 2015, A&A, 581, A45

Scalzo, R. A., Aldering, G., Antilogus, P., et al. 2010, ApJ, 713, 1073

Stebbins, J. & Kron, G. E. 1957, ApJ, 126, 266

Stritzinger, M. D., Phillips, M. M., Boldt, L. N., et al. 2011, AJ, 142, 156

Stubbs, C. W., Doherty, P., Cramer, C., et al. 2010, The Astrophysical Journal

Supplement Series, 191, 376
Stubbs, C. W. & Tonry, J. L. 2006, The Astrophysical Journal, 646, 1436
Tonry, J. L., Stubbs, C. W., Lykke, K. R., et al. 2012, ApJ, 750, 99
Tüg, H., White, N. M., & Lockwood, G. W. 1977, A&A, 61, 679
Vaz, A. L. 2011, Master's thesis, Massachusetts Institute of Technology